I/II Mixed Mode Fracture in Graphene

Bin Zhang*, Lanjv Mei

[1] State Key Laboratory of Mechanics and Control of Mechanical Structures, and College of Aerospace Engineering, Nanjing University of Aeronautics and Astronautics, Nanjing 210016, China
* Corresponding author: beenchang@nuaa.edu.cn

Abstract Nanoscale fracture of pre-cracked graphene under coupled in-plane opening and shear mechanical loading in far-field is investigated by extensive molecular dynamics simulations. Under opening-dominant loading, zigzag edge cracks grow self-similarly. Otherwise, complex mechanical stresses concentrated in the vicinity of crack tip can manipulate the direction of crack initiation changing by 30° (or multiples of 30°) to the original crack line. Toughness determined from obtained critical stress intensity factors 2.63 ~ 3.38 nN $Å^{-3/2}$ is relatively low, which demonstrates graphene is intrinsically brittle opposite to its exceptional high strength at room temperature. Graphene is easier to break along zigzag direction. Torn edges are in either zigzag or armchair manner, while zigzag edges are observed prevalently, and armchair edges are formed occasionally under particular loading conditions. Crack kinking is related to the proportion of opening and shear components of loading, and topological defects frequently appear at turning points. Our theoretical results indicate that cracking of graphene has a dependence on local mechanical stresses, edge energy and dynamic effects, which provide a possible way to regulate the edge structure of graphene.

Keywords Graphene, Crack kinking, Stress intensity factor, Molecular dynamics

1. Introduction

Graphene, as an atomic monolayer of graphite, is extensively studied after successful laboratory exfoliation [1], and it has attracted significant attention from the scientific community for its remarkable mechanical and electrical properties that are currently being explored for a number of applications including nanoelectromechanical systems, nano-electronics, *etc*. Recent mechanical experiments have shown that graphene is the strongest material measured hitherto with an elastic modulus of 1.0 TPa [2], which exceeds those of any previously existing materials. Rafiee et al. also reported that graphene as reinforcement has extraordinary effectiveness to resist fracture and fatigue in composites [3]. However, Hashimoto et al. [4] have provided a direct experimental evidence for the existence of defects in graphene layers. The extraordinary mechanical properties can be affected by the presence of defects that cause a more reduction of the strength. The existing works have treated defects in graphene as cracks that can initiate fracture.

The research on fracture of graphene can date back to the simulations conducted by Omeltchenko et al. [5], in which a notched graphite sheet was loaded uniaxial tension and then underwent cleavage. However, that retention of the cutoff function of early version potential makes the quantitative aspects of results questionable. Recently, Belytschko et al. [6-8] carried out series of theoretical researches on the fracture of pre-cracked graphene under uniaxial tensile loading. The critical stress intensity factors under pure opening loading were obtained for zigzag and armchair cracks, while the propagation direction was manually specified. Lu et al. [9] also investigated fracture of graphene nano-ribbons (GNRs) under uniaxial tension. Furthermore, shear deformation plays an important role in the wrinkling and rippling behavior of graphene, which, in turn, controls charge carrier scattering and electron mobility [10]. It is even possible to modulate the graphene energy-gap from 0.0 to 0.9 eV by combining shear deformations with uniaxial strains [11]. In point

of fact, mixed-mode fracture inevitably occurred during the tearing of graphene sheets from graphite or other substrates to obtain free-standing sheets or narrow ribbons [12]. In [5], multiple crack branched sprouting off the primary crack front, thus tilted cracks were actually under mixed tensile and shear loading. Besides theoretical studies, Kim et al. [13] presented investigations on tears in suspended monolayer graphene membranes by high-resolution transmission electron microscopy (HRTEM). However, radiation damage by electron-beam energy and applied dose cannot be neglected for light element materials due to the limitations of HRTEM [14]. It is still a challenge to observe experimentally the cracking of graphene under pure mechanical loading without electromechanical coupling effects.

Thus far, complex mechanical loading is rarely considered in previous works on fracture in graphene. Here we will show our extensive molecular dynamics (MD) simulations on nanoscale fracture of graphene under coupled opening and in-plane shear loading of far-field (I/II mixed-mode fracture). A boundary layer model embedded with a straight crack along either zigzag (ZZ) or armchair (AC) edge is applied with complex stresses by a displacement boundary governed by crack-tip asymptotic solution. The modified second-generation reactive empirical bond-order (REBO) potential [15] is used by shifting the cut-off distance and removing cut-off function to avoid unphysical dramatic increase in the interatomic force. The evolution of atomically cleaving of graphene is then revealed without manually specified direction of crack propagation.

2. Methodology and model

The well established REBO potential for hydrocarbons has been widely used [5, 9, 16-18] to specifically describe the interatomic interaction of carbon atoms lattices and nonlocal effects via an analytic function, Lennard-Jones 6-12 potential was used to mimic the nonbonding interatomic interaction, and the potential can correctly describe the bond breaking and switching between carbon atoms. In REBO potential, two cutoff distances 1.7 Å and 2.0 Å are initially set for a smooth transition of cutoff function from 1 to 0 to limit the range of covalent interactions as the interatomic distance increases. However, as noted in several previous studies [19, 20], such a cutoff function generates spurious bond forces near the cutoff distance, which will lead to unphysical results due to discontinuity in the second derivative of the cutoff function. This artifact defect shall be avoided in the study of graphene fracture. In this study, the cutoff function is taken to be 1.0 within a cutoff distance of 1.92 Å [21] and zero otherwise, as suggested by the developers [19]. It was found that the numerical results up to fracture of GNRs are unaffected if the cutoff distance is within 1.9 Å to 2.2 Å [9].

A size-reduced model containing a small circular-shaped domain cut from the crack tip is utilized to model semi-infinite cracks in real graphene. A reasonable domain size is chosen so that its outer boundary falls in the *K*-dominant zone, which can make all-atom simulations computationally efficient. We consider an initially straight crack subject to in-plane opening and shear loading characterized by the local stress intensity factor (SIF) *K* field. Two prevalent cracks with orientations along ZZ or AC edges are chosen in Figure 1. Two or three rows of atoms are removed to generate cracks in our models, and the distance between two crack surfaces is big enough to

avoid self sealing, especially in pure shear case. The length of crack is more than 10 times lattice spacing to avoid unphysical Griffith fracture stress and flaw insensitiveness [22]. A total of around 4000 carbon atoms in our disk models with a radius r = 60Å are initially relaxed until the energy of the system is fully minimized for a specified temperature. The thickness of graphene is assumed to be 3.335Å under plane stress condition. Hereafter our results are divided by 3.335Å to make connection of a two-dimensional lattice with a three-dimensional solid.

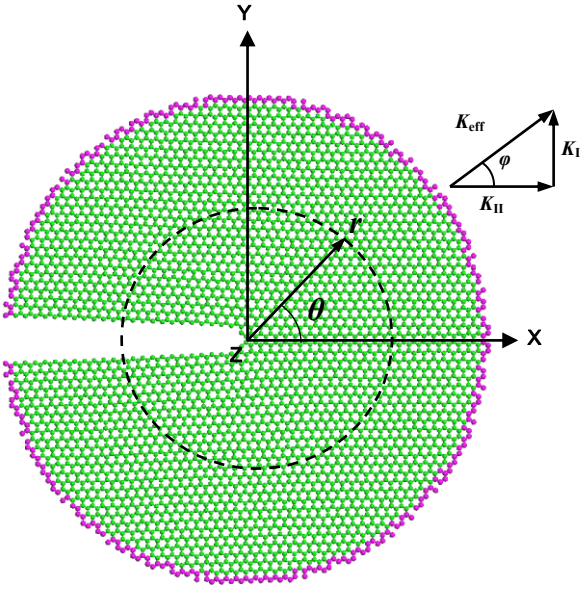

Figure 1. Boundary layer MD model and coordinates. A pre-existing straight crack along zigzag edge is embedded in a two-dimensional graphene lattice (green). The outer boundary layer (pink atoms) is subject to displacement loadings.

Williams [23] has given the asymptotic expansion of the displacement field around the crack tip in an isotropic linear elastic body. At a given SIF K^{app} applied by far-field loadings, the crack-tip asymptotic solution is as [24]

$$u_{\text{x}} = \frac{1+v}{E}\sqrt{\frac{r}{2\pi}}\left[K_{\text{I}}^{app}\cos\frac{\theta}{2}\left(k-1+2\sin^2\frac{\theta}{2}\right)+K_{\text{II}}^{app}\sin\frac{\theta}{2}\left(k+1+2\cos^2\frac{\theta}{2}\right)\right], \tag{1}$$

$$u_{\text{y}} = \frac{1+v}{E}\sqrt{\frac{r}{2\pi}}\left[K_{\text{I}}^{app}\sin\frac{\theta}{2}\left(k+1-2\cos^2\frac{\theta}{2}\right)-K_{\text{II}}^{app}\cos\frac{\theta}{2}\left(k-1-2\sin^2\frac{\theta}{2}\right)\right]. \tag{2}$$

where radius r and polar angle θ are defined in Figure 1, u_{x} and u_{y} are displacements in X and Y directions, respectively. Young's modulus E is 1.0 TPa [2], and Poisson's ratio v is 0.165 [25], and $k = (3\text{-}v)/(1+v)$ for plane stress here. $K_{\text{I}}^{\text{app}}$ and $K_{\text{II}}^{\text{app}}$ are SIF components specified by opening and shear stresses. Phase angle φ (loading mixed parameter or equivalent crack angle) is defined as $\varphi = \tan^{-1}(K_{\text{I}}^{\text{app}}/K_{\text{II}}^{\text{app}})$, and an effective SIF at the initial crack length is evaluated as $(K_{\text{eff}}^{\text{app}})^2 = (K_{\text{I}}^{\text{app}})^2 + (K_{\text{II}}^{\text{app}})^2$, see Figure 1. Therefore the far field behavior of pristine graphene is assumed to be well-represented by the solution since the singularity decreases apart from the crack tip. The boundary condition is similar to a suspended graphene spanning a hole in the TEM grid.

Mixed-mode loading in classical fracture mechanics is then imposed by initially assigning all atoms in the displacement field given by the crack-tip asymptotic solution of a specified initial $K_{\text{eff}}^{\text{app}}$. In Figure 1, atoms (pink) on the outer boundary layer are held fixed, while all the other atoms (green) are set free, and the atomic configuration is then relaxed. Then we implement the deformation-control method by applying displacement increments gradually to the fixed boundary layer separately every 500 MD steps. At each applied loading, the statically equilibrium lattice structure is calculated to minimize the total energy by the limited memory BFGS geometry optimization algorithm [26], thereby local energy minimum configurations are obtained. The velocity-Verlet time stepping scheme is used with a time step 1.0 fs at predominantly 300K with a Berendsen thermostat, and this yields a strain rate 0.0002 ps^{-1} primarily. We note that MD simulations are often sensitive to the temperature control and the loading rate, thus our results mainly provide a qualitative understanding of the fracture mechanisms.

3. Results and discussion

The energy-balance criterion by Griffith is the fundamental fracture criterion for brittle continua, which states that a crack meets the critical growth condition when the net change in the total energy of the system vanishes upon crack extension by an infinitesimal distance [27]. Using the relationship between the critical SIF of Griffith K_{th}^{c} and the energy release rate (twice of the surface energy density γ_s) for linear elastic materials, one has $K_{\text{th}}^{\text{c}} = (2E\gamma_s)^{1/2}$ [24]. Since E is assumed isotropic for graphene, K_{th}^{c} will be mainly determined by γ_s. By use of γ_s = 1.041 eV/Å and 1.091 eV/Å [28, 29] for ZZ and AC cracks, we get K_{th}^{c} = 3.162 nN $\text{Å}^{-3/2}$ and 3.238 nN $\text{Å}^{-3/2}$, respectively.

Table 1. Effective critical stress intensity factors $K_{\text{eff}}^{\text{c}}$ (nN $\text{Å}^{-3/2}$) of zigzag and armchair cracks in graphene under far-field loading at various phase angles φ.

φ		0°	15°	30°	45°	60°	75°	90°	90°	90°	90°	90°	90°
$K^{\text{c}}_{\text{eff}}$	ZZ	3.06	2.75	2.63	2.90	3.15	3.02	3.05	3.16[a]	4.21[b]	2.64[c]	6.0[d]	10.32[e]
	AC	2.87	3.30	3.28	2.87	2.78	2.85	3.38	3.24[a]	3.71[b]			

[a] Critical stress intensity factor of Griffith K_{th}^{c}; [b] Ref. 6; [c] Ref. 7; [d] Ref. 5; [e] Ref. 30.

In Table 1 and Figure 2, our results show that the effective critical SIF $K_{\text{eff}}^{\text{c}}$ of I/II mixed-mode loading falls in the range between 2.63 nN $\text{Å}^{-3/2}$ and 3.38 nN $\text{Å}^{-3/2}$ varying with φ, relatively low compared to steel, which reveals that graphene is brittle at 300K opposing its ultrahigh strength. As the difference of geometric chiral angle between AC and ZZ edges is 30°, similar trends for $K_{\text{eff}}^{\text{c}}$ are observed if φ is shifted by 30°, see Figure 2. $K_{\text{eff}}^{\text{c}}$ along ZZ edges are slightly lower indicating smaller toughness, thus graphene is easier to break along ZZ direction. For ZZ cracks under pure opening tension (φ = 90°), our $K_{\text{eff}}^{\text{c}}$ are reasonable with theoretical K_{th}^{c}, and compared with available reported datum, Table 1, the discrepancy may be due to different crack models [5, 7] and potentials [6, 30].

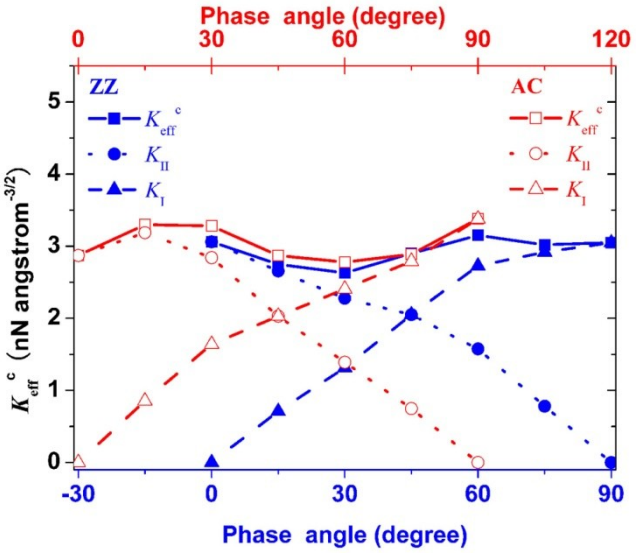

Figure 2. Effective critical stress intensity factors K_{eff}^{c} of graphene cracks, ZZ in blue and AC in red, changing with phase angles φ of far-field loading. K_I and K_{II} are opening and shear components of K_{eff}^{c}.

Up to now, no single criterion in classical continuum mechanics can give satisfactory predictions for crack initiation direction under all loading conditions. All existing criteria predict that a crack under mode II (in-pane shear, $\varphi = 0°$) loading propagates along about a 70° direction with respect to the original crack line. However, a mode II crack either propagates in mode I (opening, $\varphi = 90°$) or mode II, depending on material properties and load magnitudes [31].

Continuum criteria seem to lose efficacy in predicting direction of crack initiation in graphene. In Figure 3a-f, our results show that ZZ cracks initiate in the direction of an angle $\beta = 120°$ deviating from the original edge when in-plane shear loading is prevailing, β maintains unchanged till $\varphi = 60°$ and fresh edges are in zigzag (blue). Further increasing φ will induce the transition of β. At $\varphi = 65°$, β changes to 150°, and fresh edges are in armchair (red). This configuration coincides with the prediction that zigzag-armchair junctions with an angle of 150° would be more stable [32, 5]. Once $\varphi > 65°$, opening loading becomes dominant, crack grows self-similarly along original direction and fresh edges are in zigzag again.

For AC cracks in Figure 3g-l, initiation angle $\beta = 90°$ at $\varphi = 0°$, new crack tips nucleate prior to initial tip, and fresh edges are in zigzag. At $\varphi = 26.5°$, propagating direction changes to $\beta = 120°$, and fresh edges are in armchair. When $\varphi > 26.5°$, β transforms to 150° and keeps unchanged till $\varphi = 90°$, and fresh edges are in zigzag again.

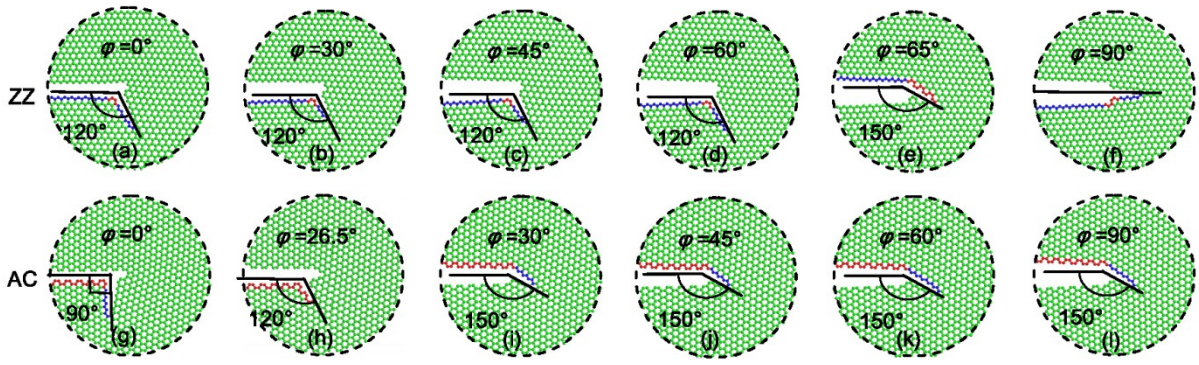

Figure 3. Insets (r = 30Å, cut from the whole models in Figure 1) of crack initiation in flawed graphene (green) under I/II mixed-mode loading. (a)-(f) ZZ cracks initiation at phase angle φ = 0°, 30°, 45°, 60°, 65°, 90°, and (g)-(l) AC cracks at φ = 0°, 26.5°, 30°, 45°, 60°, 90°, correspondingly.

Fresh edges exhibit mostly in zigzag, and armchair edges are formed during the transition of propagating direction. Under loading $K_{\text{eff}}^{\text{app}}$ = 3.21 nN Å$^{-3/2}$ at φ = 65° in Figure 3e, zigzag crack (blue) kinks and armchair edge (red) is formed. In Figure 3h, armchair crack (red) turns its direction with 120° followed by armchair edge (red) under $K_{\text{eff}}^{\text{app}}$ = 3.25 nN Å$^{-3/2}$ at φ = 26.5°. This is similar to experimental tears kinking within graphene membrane under complex mechanical stress applied by circular boundary of the Quantifoil holey carbon TEM grid [13].

With the increasing of complex loading, the stress concentrated around crack tip morphs the hexagonal carbon rings into deformed shapes. Once the bonds at the tip rotated or broken, the hexagonal symmetry of the graphene lattice is destroyed with the formation and motion of topological defects, which leads to crack kinking. The dynamic effect of a fast fracture in MD simulations can also cause kinking, while branching is not observed. Further crack extension would proceed by alternating sequence of bond breaking or rotation.

Graphene edges are of particular interest since their orientation determines the electronic properties. Crack extension with the formation of fresh edges is mainly caused by local high strain concentrated around crack tips. Our simulations demonstrate that torn edges maintain straightness and clean in either zigzag or armchair direction, in Figure 3, and can change directions by 30° or multiples of 30°, in Figure 3, coincided with experiments [13]. Under pure opening loading (φ = 90°), the growth of zigzag cracks is self-similar whereas armchair cracks advance in an irregular manner, consistent with previous reports [6]. The direction of crack growth changes definitely under coupled opening and shearing stresses and edges interconvert between ZZ and AC. Cracks preferably grow along zigzag directions in agreement with previous theoretical simulations [9, 12]. By Griffith criterion, this suggests lower edge energy in ZZ opposed to AC, which is coincided with simulations by empirical potentials [28, 29, 33]. More abundant ZZ edges appeared may be due to lower edge energy, somewhat local residual stresses and dynamic fracture effects. Experiments also showed long-term stability [34] of ZZ edges, and more ZZ edges were initially formed at high temperatures [35]. In [13], the initial torn edges were along ZZ direction under pure mechanical stress during the graphene transfer process, while heating and chemical effects, knock-on sputtering induced by electron irradiation in TEM inevitably influenced crack extension stimulated afterwards.

Another experiment [36] also confirmed that the zigzag edge is more stable than the armchair edge, although the opposite has been predicted theoretically by *ab initio* calculations which depend strongly on the choice of the density functional among different DFT calculations yielding dramatically different values in quantitative scattering.

During our simulations, total energy at each strain level is minimized for each equilibrium lattice structure. The kinematic energy changes slightly while potential energy increases gradually since the temperature is coupled with a thermostat. Energy jumps are infrequently observed, thus lattice-trapping effects are negligibly small for long-range potentials we used. Undoubtedly, temperature and strain rate can quantitatively affect K^c that increases slightly with increase of strain rates while decreases with temperature. At high temperature beyond 1000K, fracture shows plastic behaviors opposite to brittle at room temperature, the crack edges are reconstructed, fresh surfaces are bridged with carbon chains, and formation and motion of defects and vacancies appear frequently.

4. Concluding remarks

In summary, graphene embedded with pre-existing zigzag or armchair crack under complex mechanical stresses is studied by extensive molecular dynamics simulations based on the modified REBO potential. An asymptotic expansion of the displacement field in the region of crack tip is adopted to apply loading combined with in-plane opening and shear stresses. The critical effective stress intensity factors are obtained in the range of 2.63 nN $Å^{-3/2}$ to 3.38 nN $Å^{-3/2}$ varied with the phase angle of far-field loading, the predicted low toughness indicates that strong graphene is absolutely brittle at room temperature. The direction of crack initiation is also dependent on the phase angle, and changes by 30° (or multiples of 30°) to the original crack line. Straight cracks with zigzag edges grow self-similarly when opening loading is dominant, or else kinking occurred. Torn edges of fresh cracks are along either zigzag or armchair edge, while zigzag edges are more preferable. Fresh armchair edges are formed occasionally under particular stress conditions. Our theoretical results show that graphene cracking prefers along zigzag edges concerning with its lower toughness and complex mechanical stress in dynamic fracture.

Acknowledgements

The author gratefully acknowledges supports from Newton International Fellowship (NF080039) and Newton Alumni Follow-On of UK's Royal Society hosted by University of Glasgow and Newcastle University, and Aeronautical Science Foundation of China (2012ZF52074), NSFCs (10602023 and 11232007), the Fundamental Research Funds for the Central Universities, the Program for Changjiang Scholars and Innovative Research Team (IRT0968) and National Basic Research Program (973, 2011CB707602) of China.

References

[1]. K.S. Novoselov, A.K. Geim, S.V. Morozov, D. Jiang, Y. Zhang, S.V. Dubonos, I.V. Grigorieva, and A.A. Firsov, Electric field effect in atomically thin carbon films. Science, 306(5696) (2004) 666 -669.

[2]. C. Lee, X. Wei, J.W. Kysar, and J. Hone, Measurement of the elastic properties and intrinsic strength of

monolayer graphene. Science, 321(5887) (2008) 385 -388.

[3]. M.A. Rafiee, J. Rafiee, I. Srivastava, Z. Wang, H. Song, Z. Yu, and N. Koratkar, Fracture and fatigue in graphene nanocomposites. Small, 6(2) (2010) 179-183.

[4]. A. Hashimoto, K. Suenaga, A. Gloter, K. Urita, and S. Iijima, Direct evidence for atomic defects in graphene layers. Nature, 430(7002) (2004) 870-873.

[5]. A. Omeltchenko, J. Yu, R.K. Kalia, and P. Vashishta, Crack front propagation and fracture in a graphite sheet: a molecular-dynamics study on parallel computers. Phys Rev Lett, 78(11) (1997) 2148-2151.

[6]. M. Xu, A. Tabarraei, J.T. Paci, J. Oswald, and T. Belytschko, A coupled quantum/continuum mechanics study of graphene fracture. Int J Fracture, 173(2) (2012) 163-173.

[7]. S. Zhang, T. Zhu and T. Belytschko, Atomistic and multiscale analyses of brittle fracture in crystal lattices. Phys Rev B, 76(9) (2007) 094114.

[8]. S. Huang, S. Zhang, T. Belytschko, S.S. Terdalkar, and T. Zhu, Mechanics of nanocrack: fracture, dislocation emission, and amorphization. J Mech Phys Solids, 57(5) (2009) 840-850.

[9]. Q. Lu, W. Gao and R. Huang, Atomistic simulation and continuum modeling of graphene nanoribbons under uniaxial tension. Mod Simul Mater Sci Eng, 19 (2011) 054006.

[10]. M.I. Katsnelson and A.K. Geim, Electron scattering on microscopic corrugations in graphene. Phil Trans R Soc A, 366(1863) (2008.) 195-204.

[11]. G. Cocco, E. Cadelano and L. Colombo, Gap opening in graphene by shear strain. Phys Rev B, 81(24) (2010) 241412.

[12]. D. Sen, K.S. Novoselov, P.M. Reis, and M.J. Buehler, Tearing graphene sheets from adhesive substrates produces tapered nanoribbons. Small, 6(10) (2010) 1108-1116.

[13]. K. Kim, V.I. Artyukhov, W. Regan, Y. Liu, M.F. Crommie, B.I. Yakobson, and A. Zettl, Ripping graphene: preferred directions. Nano Lett., 12(1) (2012) 293-297.

[14]. J.C. Meyer, F. Eder, S. Kurasch, V. Skakalova, J. Kotakoski, H.J. Park, S. Roth, A. Chuvilin, S. Eyhusen, G. Benner, A.V. Krasheninnikov, and K. U., 14. Phys Rev Lett, 108(19) (2012) 196102.

[15]. D.W. Brenner, O.A. Shenderova, J.A. Harrison, S.J. Stuart, B. Ni, and S.B. Sinnott, A second-generation reactive empirical bond order (rebo) potential energy expression for hydrocarbons. J Phys Cond Mat, 14 (2002) 783.

[16]. B. Zhang and W. Guo, Cracking diamond anvil cells by compressed nanographite sheets near the contact edge. Appl Phys Lett, 87 (2005) 051907.

[17]. B. Zhang, Y. Liang and H. Sun. Structural phase transition and failure of nanographite sheets under high pressure: a molecular dynamics study. Journal of Physics: Condensed Matter, 19 (2007) 346224.

[18]. B. Zhang, L.Mei and H. F Xiao. Nanofracture in graphene under complex mechanical stresses. Applied Physics Letters, 101(12) (2012) 121915

[19]. O.A. Shenderova, D.W. Brenner, A. Omeltchenko, X. Su, and L.H. Yang, Atomistic modeling of the fracture of polycrystalline diamond. Phys Rev B, 61(6) (2000) 3877.

[20]. T. Belytschko, S.P. Xiao, G.C. Schatz, and R. Ruoff, Atomistic simulations of nanotube fracture. Phys Rev B, 65 (2002) 235430

[21]. R. Grantab, V.B. Shenoy and R.S. Ruoff, Anomalous strength characteristics of tilt grain boundaries in graphene. Science, 330(6006) (2010) 946-948.

[22]. H. Gao, B. Ji, I.L. J A Ger, E. Arzt, and P. Fratzl, Materials become insensitive to flaws at nanoscale: lessons from nature. Proc Natl Acad Sci USA, 100(10) (2003) 5597.

[23]. M.L. Williams, On the stress distribution at the base of a stationary crack. J Appl Mech, 24(1) (1957) 109-114.

[24]. T.L. Anderson, Fracture mechanics: fundamentals and applications. 2 ed, CRC Press, Boca Raton, FL, 1991

[25]. O.L. Blakslee, D.G. Proctor, E.J. Seldin, G.B. Spence, and T. Weng, Elastic constants of compression-annealed pyrolytic graphite. J Appl Phys, 41(8) (1970) 3373-3382.
[26]. D.C. Liu and J. Nocedal, On the limited memory bfgs method for large scale optimization. Math Program, 45(1) (1989) 503-528.
[27]. A.A. Griffith, The phenomena of rupture and flow in solids. Philos Trans R Soc London Ser A, 221 (1921) 163-198.
[28]. Q. Lu and R. Huang, Excess energy and deformation along free edges of graphene nanoribbons. Phys Rev B, 81(15) (2010) 155410.
[29]. P.S. Branicio, M.H. Jhon, C.K. Gan, and D.J. Srolovitz, Properties on the edge: graphene edge energies, edge stresses, edge warping, and the wulff shape of graphene flakes. Mod Simul Mater Sci Eng, 19 (2011) 054002.
[30]. S.S. Terdalkar, S. Huang, H. Yuan, J.J. Rencis, T. Zhu, and S. Zhang, Nanoscale fracture in graphene. Chem Phys Lett, 494(4) (2010) 218-222.
[31]. J. Qian and A. Fatemi, Mixed mode fatigue crack growth: a literature survey. Eng Fract Mech, 55(6) (1996) 969-990.
[32]. M. Engelund, J.A. F U Rst, A.P. Jauho, and M. Brandbyge, Localized edge vibrations and edge reconstruction by joule heating in graphene nanostructures. Phys Rev Lett, 104(3) (2010) 036807.
[33]. V.B. Shenoy, C.D. Reddy, A. Ramasubramaniam, and Y.W. Zhang, Edge-stress-induced warping of graphene sheets and nanoribbons. Phys Rev Lett, 101(24) (2008) 245501.
[34]. Ç. Ö. Girit, J.C. Meyer, R. Erni, M.D. Rossell, C. Kisielowski, L. Yang, C.H. Park, M.F. Crommie, M.L. Cohen, S.G. Louie, and Others, Graphene at the edge: stability and dynamics. Science, 323(5922) (2009) 1705-1708.
[35]. X. Jia, M. Hofmann, V. Meunier, B.G. Sumpter, J. Campos-Delgado, J.M. Romo-Herrera, H. Son, Y.P. Hsieh, A. Reina, J. Kong, and Others, Controlled formation of sharp zigzag and armchair edges in graphitic nanoribbons. Science, 323(5922) (2009) 1701-1705.
[36]. Y.C. Cheng, H.T. Wang, Z.Y. Zhu, Y.H. Zhu, Y. Han, X.X. Zhang, and U. Schwingenschl O Gl, Strain-activated edge reconstruction of graphene nanoribbons. Phys Rev B, 85(7) (2012) 073406.